SCIENCE CHINA
Earth Sciences

•PERSPECTIVE•

April 2025 Vol.68 No.4: 1298–1302
https://doi.org/10.1007/s11430-024-1533-7

Causes and predictability of the "explosive" intensification of Super Typhoon Yagi after entering the South China Sea in 2024

Ruifen ZHAN[1,2] & Jie FENG[1,3*]

1. Department of Atmospheric and Oceanic Sciences/Institute of Atmospheric Sciences, Fudan University, Shanghai 200438, China
2. CMA-FDU Joint Laboratory of Marine Meteorology, Shanghai 210044, China
3. Shanghai Key Laboratory of Ocean-land-atmosphere Boundary Dynamics and Climate Change, Shanghai 200438, China

Received December 6, 2024; revised February 11, 2025; accepted February 24, 2025; published online March 7, 2025

Citation: Zhan R, Feng J. 2025. Causes and predictability of the "explosive" intensification of Super Typhoon Yagi after entering the South China Sea in 2024. Science China Earth Sciences, 68(4): 1298–1302, https://doi.org/10.1007/s11430-024-1533-7

1. Introduction

The intensification of nearshore tropical cyclones (TCs), particularly the process of rapid intensification (RI), poses a severe threat to coastal populations due to its short warning time and devastating impact. It also presents a significant challenge to operational TC forecasting. Therefore, understanding the physical mechanisms and predictability of nearshore TC intensification is of great importance. However, due to the complex interactions among multi-scale dynamic and physical processes involved in TC intensity changes, the physical mechanisms governing nearshore TC intensification, especially RI, remain insufficiently understood.

In 2024, Super Typhoon Yagi (the 11th named TC of the year) exhibited an extraordinary episode of "explosive" intensification after entering the South China Sea, characterized by a remarkable surge in intensity within a short period. In just 15 h, Yagi underwent a three-stage intensification sequence from a Typhoon to a Severe Typhoon and then to a Super Typhoon. Notably, Yagi experienced three successive RI events near the coast (as defined by Li et al. (2021), where RI is characterized by a 12-h intensification rate exceeding 8 m s^{-1}), ultimately maintaining super typhoon intensity for 64 h, setting a record for the longest sustained intensification of a TC in the South China Sea since records began in 1949. Such an event is exceptionally rare.

Moreover, after its formation, Yagi traveled westward and made four landfalls across three countries, with the last three landfalls occurring at Super Typhoon intensity (Figure 1a). The TC's extensive track and prolonged strength led to widespread and severe impacts. Given the unusual nature of this nearshore TC event, this study aims to investigate the underlying mechanisms driving Yagi's persistent intensification after entering the South China Sea and assess its predictability.

2. Results

2.1 Possible mechanisms of rapid intensification in TC Yagi

After entering the South China Sea, TC Yagi underwent three RI events: the first RI began at 12:00 UTC on September 3, lasting 24 h, during which the intensity increased from 25 to 58 m s^{-1}, a rise of 33 m s^{-1}; the second RI started at 09:00 UTC on September 5, lasting two stages, with intensity increasing from 58 m s^{-1} to its peak of 68 m s^{-1}, a rise of 10 m s^{-1}; after making landfall in Hainan, Yagi experienced a brief weakening and then started its third RI at 18:00 UTC on September 6, where it strengthened from 52 to 60 m s^{-1}, increasing 8 m s^{-1}, reaching the second peak intensity of its entire lifecycle.

These three RI events exhibited significant differences in

* Corresponding author (email: fengjiefj@fudan.edu.cn)

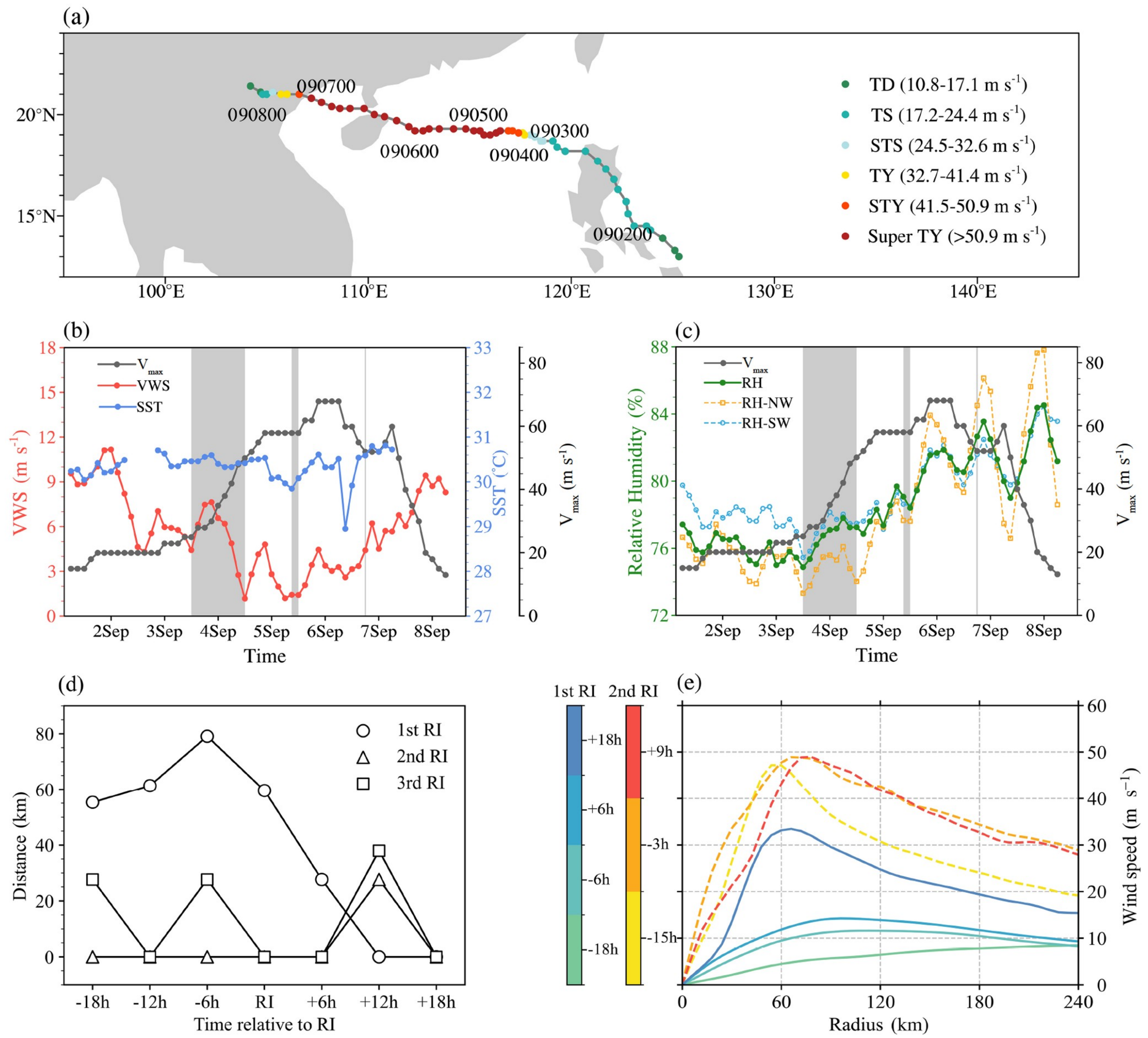

Figure 1 Track, intensity, environmental factors, and time series of vortex tilt magnitude and the mean radial profile of tangential wind before and after RI for Super Typhoon Yagi. (a) TC track. (b) Maximum wind speed (V_{max}, black line, right y-axis), vertical wind shear (VWS, red line, left y-axis) calculated as $\mathrm{VWS}=\sqrt{\left(U_{200}-U_{850}\right)^2+\left(V_{200}-V_{850}\right)^2}$ within the 200–850 hPa layer in the 200–800 km annular region around the TC center, and sea surface temperature (SST, °C, blue line, right y-axis) within a 3° radius of the TC center. (c) Filtered relative humidity (RH, %) in the 850–700 hPa layer within a 10° radius of the TC center (green, left y-axis), with mean values in the northwest quadrant (orange) and southwest quadrant (blue). In (b) and (c), the gray shaded boxes (lines) indicate the timing of RI events. (d) Vortex tilt magnitude (km), defined as the distance between the surface circulation center (mean sea level pressure) and the mid-level circulation center (500 hPa geopotential height). (e) Mean radial profile of 10-m tangential wind (m s^{-1}) before and after RI, where solid lines represent the first RI event, and dashed lines represent the second RI event. TC data are obtained from the China Meteorological Administration (CMA), while environmental data are sourced from the ECMWF ERA5 reanalysis.

intensity and duration. The first RI lasted the longest and can be considered a "marathon-type" RI (consisting of at least eight consecutive overlapping RI stages), while the latter two RIs were shorter in duration, especially the third RI, which was the shortest and was completed within just 6 h, thus categorized as a "sprint-type" RI (at most four consecutive overlapping RI stages; Judt et al., 2023). It is worth noting that the "sprint-type" RI in this study is not entirely consistent with the classification proposed by Judt et al. (2023), as their classification was limited to early-stage vortex convection, whereas we extend it to different phases of TC development. These findings indicate that the ability of Yagi to maintain Super Typhoon intensity for 64 h was closely linked to the occurrence of these three RI events.

The possible reasons for these three RI events will be examined based on environmental factors, wind field structure, and inner-core dynamic characteristics. Figure 1b and 1c present the environmental factors near the TC center throughout its lifecycle, including sea surface temperature (SST), environmental vertical wind shear, and low-level environmental relative humidity. It is evident that Yagi remained over high SST waters (ranging from 30°C to 31°C) throughout its lifetime, with a notable SST increase 3 h before the third RI, which may be attributed to Yagi crossing the relatively cool Qiongzhou Strait and entering the warmer Beibu Gulf. The evolution of environmental vertical wind shear exhibited different characteristics across different stages: one day before the first RI, Yagi was under moderate shear, which significantly decreased during the later stages of RI, possibly associated with the vertical alignment of the TC vortex (Figure 1d). One day before the second RI, Yagi was under weak shear conditions, which further decreased to nearly 1 m s^{-1} after the RI began, during which the TC axis was nearly upright, favoring the accumulation of inner-core energy (convective latent heat release) and the rapid intensification of the warm core. When the third RI began, vertical wind shear slightly increased.

Low-level humidity remained above 75% throughout the process, slightly higher than the 74% climatological mean of all RI cases from 1989 to 2006 (Kaplan et al., 2010), suggesting favorable conditions for RI. In particular, the third RI occurred under the highest humidity conditions, exceeding 80%. Furthermore, we calculated relative humidity within a 1000 km radius of the TC center in the northwest and southwest quadrants—the former representing the intrusion of cold and dry northern air, and the latter indicating monsoonal inflow (Figure 1c). Before the first RI, despite weak cold air intrusion in the northwest quadrant, the continuous influx of warm, moist monsoonal air from the southwest provided ample moisture and convective available potential energy (CAPE), facilitating the rapid intensification of the TC. Prior to the second and third RIs, relative humidity in the northwest quadrant increased, and monsoonal activity intensified, further enhancing moisture transport. Combined with the increase in SST, these factors contributed to the eruption of inner-core convection, ultimately leading to rapid intensification.

The contraction of the radius of maximum wind (RMW) and the reduction in vertical vortex tilt are favorable conditions for RI (Rogers et al., 2015; Rios-Berrios et al., 2018). Figure 1d and 1e illustrate the evolution of the displacement between the surface and mid-tropospheric centers (indicating the degree of tilt) over time, as well as changes in the tangential wind radial profile before and after the first two RI events. 18 h before the first RI until its onset, the wind profile evolved gradually, and the vortex exhibited significant vertical tilt. 6 h before RI, the mid-level center was displaced 80 km from the surface center, consistent with the TC's slow intensification. However, within 6 h after RI onset, vortex tilt rapidly decreased, and the wind profile indicated rapid inner-core contraction and intensification. Specifically, from 12 to 18 h into RI, the RMW contracted from 100 to 60 km, and the surface and mid-level centers became nearly aligned, exhibiting the typical characteristics of RI. This vertical alignment marked the establishment of a strong warm core, increased eyewall heating efficiency, and enhanced subsidence warming within the eye, leading to a rapid drop in sea level pressure and intensification of the TC.

The second and third RIs displayed different structural characteristics. The wind profiles remained relatively stable, with no significant structural changes, and the vortex was nearly vertically aligned, indicating a well-organized TC structure with sufficient inner-core energy. Due to the small inner-core scale, the high inertial stability of the eyewall enhanced heating efficiency, further facilitating intensification (Wang and Wang, 2013). However, radar observations (not shown) revealed that 3 h before the third RI, Yagi developed a concentric eyewall structure. Owing to favorable environmental conditions (Figure 1b and 1c), both inner and outer eyewalls intensified simultaneously at the onset of RI. As the TC moved westward, portions of the outer eyewall made landfall, gradually transforming the annular convective structure into an open outer rainband. The dissipation of the outer eyewall accelerated the development of the inner eyewall, leading to momentum and moisture convergence toward the inner-core region. Consequently, from 12:00 to 13:00 UTC on September 7, Yagi's intensity surged by 5 m s^{-1}, reaching its second peak.

Overall, the three RI events in TC Yagi were driven by a combination of environmental and dynamic factors. High SSTs provided the necessary oceanic heat flux, while sustained warm and moist monsoonal inflow overcame the negative impact of cold air intrusion from the northwest and supplied continuous moisture and energy for inner-core convection. The reduction in vertical wind shear facilitated vertical alignment, enabling the establishment and rapid intensification of the warm core, which was the key thermodynamic mechanism triggering the first RI. The second RI was mainly driven by high SSTs, increased moisture, and further reduction in vertical wind shear, while the third RI was supported by high SSTs, ample moisture supply, weak vertical wind shear, and high inner-core inertial stability. Additionally, the formation and dissipation of a concentric eyewall structure further enhanced the inner-core development, leading to the third short-duration RI. The combined influence of these factors allowed Yagi to maintain super typhoon intensity for 64 h.

2.2 Predictability of the intensification process of TC Yagi

The three RI events of TC Yagi exhibited unique characteristics and were the primary reasons for its prolonged maintenance as a Super Typhoon over the South China Sea. A question arises as to whether numerical forecasts can reasonably predict these processes.

Previous studies have explored the predictability of TC RI (Judt and Chen, 2016), but these studies did not distinguish between different types of RI. Here, we examine the TC intensity forecasts from the Shanghai Typhoon Institute's Regional Typhoon Integrated (9 km) Ensemble Prediction System, SWARMS-EN, which consists of 20 ensemble members, to assess the predictability of the three RI events. The system is based on the WRF model and has optimized physical parameterization schemes for TC intensity forecasting. It is important to note that the 9 km ensemble system cannot resolve the fine structures of the TC inner core, and this study focuses only on the uncertainty distribution among different ensemble members and how well the model captures the likelihood of RI occurrence.

Our evaluation indicates that this system performed better in predicting the intensity of TC Yagi compared with other global ensemble prediction systems (Figure 2). For the intensity change during the first RI's initial 12 h, the SWARMS-EN system demonstrated some predictive capability, with 40%, 35%, and 25% of the ensemble members capturing the RI process within 12 h when initialized 48, 24, and 12 h in advance, respectively. However, the model's ability to predict the continuous 24-h RI process starting at 12:00 UTC on September 3 significantly declined. None of the ensemble members initialized 24 and 12 h in advance could predict the continuous 24-h RI, while 20% of the members initialized 48 h in advance captured it. This suggests that the model may have some predictive skill in forecasting Yagi's marathon-type RI process. When initialized from a weaker tropical storm, the forecast system had a more accurate initial vortex intensity and allowed more time for the TC to adjust and strengthen dynamically within the model, leading to more accurate predictions of the RI process compared with forecasts initialized during the TC stage (Feng and Wang, 2021). The second RI lasted only two stages, and the ensemble prediction system exhibited no skill in forecasting the RI process for different lead times, with an overall intensity prediction error reaching 10 m s^{-1}. This could be primarily due to the lack of high-quality observations near the TC eyewall when Yagi was already at the strong TC stage, leading to significant underestimation of TC intensity in the model's initial conditions (Feng and Wang, 2019; Feng et al., 2022). The third RI lasted even shorter, and the model's prediction skill was even lower. Almost all ensemble members forecasted that the TC's intensity would either remain constant or decrease.

The predictability results of these three RI events suggest that the prolonged maintenance of TC intensity and the multiple RI processes during this period may have low predictability, with the sprint-type RI exhibiting the lowest predictability.

3. Discussion

Studies have shown an increasing trend in nearshore TC RI events under global warming (Li et al., 2023; Li et al., 2024). Undoubtedly, this poses greater challenges for TC intensity forecasting. In future forecasts of multiple RI events, besides considering environmental factors such as high SST, sustained monsoonal moisture transport, and weakened vertical wind shear, special attention should also be paid to the evolution of internal dynamic structures, such as the reduction in TC tilt, the enhancement of warm-core heating efficiency, and eyewall replacement processes. Additionally, an important direction for future research is improving TC intensity forecasts by integrating numerical simulations with machine learning methods tailored for different types of RI events.

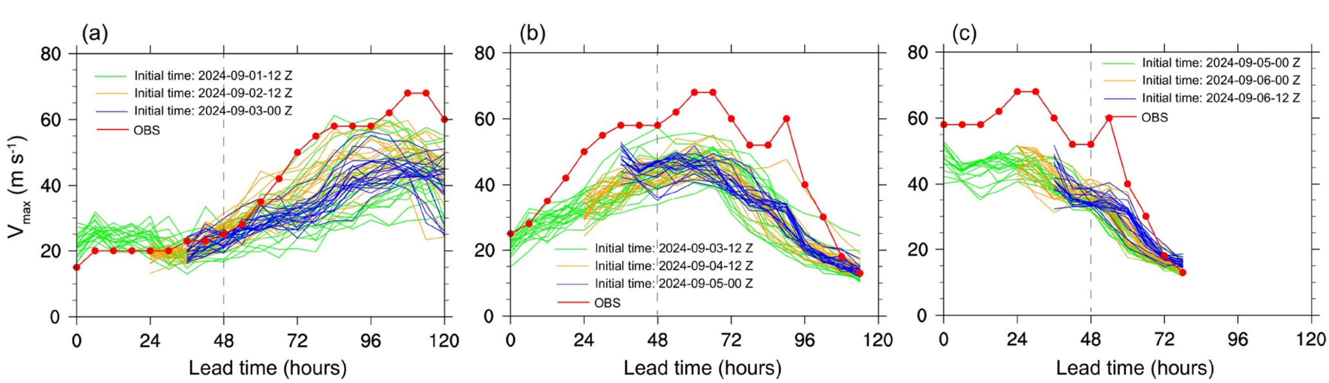

Figure 2 Ensemble forecasts of TC Yagi's intensity. The onset times of the three RI events are indicated by vertical gray dashed lines. (a) For the first RI, the three forecast initialization times are 2024-09-01 12:00 (green), 2024-09-02 12:00 (orange), and 2024-09-03 00:00 (blue). (b) For the second RI, the three forecast initialization times are 2024-09-03 12:00 (green), 2024-09-04 12:00 (orange), and 2024-09-05 00:00 (blue). (c) For the third RI, the three forecast initialization times are 2024-09-05 00:00 (green), 2024-09-06 00:00 (orange), and 2024-09-06 12:00 (blue). The red solid line represents the observed intensity.

Acknowledgements *We sincerely thank Professor Yuqing WANG for valuable suggestions, Dr. Dajun ZHAO and Dr. Qian WANG for providing some observational data, and Researcher Wei HUANG for supplying TC forecasts from the SWARMS-EN operational ensemble prediction system. This work was supported by the National Natural Science Foundation of China Basic Science Center Project (Grant No. 42288101) and the Shanghai Science and Technology Committee Project (Grant No. 23DZ1204703).*

Conflict of interest The authors declare that they have no conflict of interest.

References

Feng J, Wang X. 2019. Impact of assimilating upper-level dropsonde observations collected during the TCI field campaign on the prediction of intensity and structure of Hurricane Patricia (2015). Mon Weather Rev, 147: 3069–3089

Feng J, Wang X. 2021. Impact of increasing horizontal and vertical resolution during the HWRF Hybrid EnVar Data assimilation on the analysis and prediction of Hurricane Patricia (2015). Mon Weather Rev, 149: 419–441

Feng J, Qin X, Wu C, Zhang P, Yang L, Shen X, Han W, Liu Y. 2022. Improving typhoon predictions by assimilating the retrieval of atmospheric temperature profiles from the FengYun-4A's Geostationary Interferometric Infrared Sounder (GIIRS). Atmos Res, 280: 106391

Judt F, Chen S S. 2016. Predictability and dynamics of tropical cyclone rapid intensification deduced from high-resolution stochastic ensembles. Mon Weather Rev, 144: 4395–4420

Judt F, Rios-Berrios R, Bryan G H. 2023. Marathon versus sprint: Two modes of tropical cyclone rapid intensification in a global convection-permitting simulation. Mon Weather Rev, 151: 2683–2699

Kaplan J, Demaria M, Knaff J A. 2010. A revised tropical cyclone rapid intensification index for the Atlantic and Eastern North Pacific Basins. Weather Forecasting, 25: 220–241

Li X, Zhan R, Wang Y, Xu J. 2021. Factors controlling tropical cyclone intensification over the marginal seas of China. Front Earth Sci, 9: 795186

Li X, Zhan R, Wang Y, Zhao J, Ding Y, Song K. 2024. Recent increase in rapid intensification events of tropical cyclones along China coast. Clim Dyn, 62: 331–344

Li Y, Tang Y, Wang S, Toumi R, Song X, Wang Q. 2023. Recent increases in tropical cyclone rapid intensification events in global offshore regions. Nat Commun, 14: 5167

Rios-Berrios R, Davis C A, Torn R D. 2018. A hypothesis for the intensification of tropical cyclones under moderate vertical wind shear. J Atmos Sci, 75: 4149–4173

Rogers R F, Reasor P D, Zhang J A. 2015. Multiscale structure and evolution of Hurricane Earl (2010) during rapid intensification. Mon Weather Rev, 143: 536–562

Wang Y, Wang H. 2013. The inner-core size increase of Typhoon Megi (2010) during its rapid intensification phase. Trop Cycl Res Rev, 2: 65–80

(Editorial handling: Guixing CHEN)